PHYSICAL REVIEW C VOLUME 15, NUMBER 6 JUNE 1977

Shapes of heavy transition nuclei in a self-consistent anisotropic oscillator model

D. Goss
Department of Physics and Astronomy, Nebraska Wesleyan University, Lincoln, Nebraska 68504
(Received 9 November 1976)

The second- and fourth-order mass moments of the even-neutron transition nuclei $^{178-188}$W, $^{182-194}$Os, $^{187-195}$Ir, $^{186-198}$Pt, $^{191-199}$Au, and $^{194-206}$Hg have been calculated using a self-consistent version of the anisotropic oscillator model. A structural basis is found for possible asymmetric intrinsic nuclear shapes in the transition region, particularly in some of the Os and Pt nuclei and the Ir and Au nuclei nearest to even neighbors with large deformations. The calculations predict large negative fourth-order moments for this region.

PACS numbers: 21.60.Ev, 27.70.+q, 27.80.+w

[NUCLEAR STRUCTURE Calculated Q_{20}, Q_{22}, Q_{40}, Q_{42}, Q_{44}, β_2, γ, and β_4 in anisotropic oscillator model for heavy transition nuclei.]

I. INTRODUCTION

Several groups[1,2] have recently shown that semiquantitative fits may be obtained to the energy levels of nuclei in the transition (W to Pb) region by using an asymmetric rotor model of the even-A nuclei. Neighboring odd nuclei are treated as a particle or hole coupled to the even core by a potential with second order deformation:

$$V_2 = -k_2\beta_2[(\cos\gamma)Y_{20}+(\sin\gamma/\sqrt{2}) \times(Y_{22}+Y_{2,-2})] \quad (1)$$

The inclusion of fourth-order terms in the potential

$$V_4 = -k_2[\beta_4 Y_{40} +a_{42}(Y_{42}+Y_{4,-2}) +a_{44}(Y_{44}+Y_{4,-4})] \quad (2)$$

(at least the axial term) has been found to be at least as important as axial asymmetry for good fits to the energy levels[3].

One of the unresolved questions regarding these nuclei is the structural origin of non-axial deformations[1]. Microscopic calculations using a model interaction[4] show no deep minima corresponding to the stable non-axial deformation inferred for an asymmetric rotor. Similar results have been found using a non-axial Nilsson[5] model[6], the Nilsson model with pairing[7], and with a modification of the Strutinsky shell-correction technique applied to a deformed Woods-Saxon well potential[8]. The current method of determining γ combines the empirical relation between β_2 and the moment of inertia and the experimental 0^+-2^+ spacing with the asymmetric rotor formula for the spacing[1,9], so that it has no structural basis. There is thus a gap between the empirical and the structural descriptions of these nuclei.

The most accurate means of determining the intrinsic shapes of nuclei is probably an unrestricted deformed Hartree-Fock (HF) calculation using a "realistic" interaction. It is clear that this would be a formidable undertaking, particularly if many spherical shells are taken into account. Hartree-Fock calculations using a deformed oscillator basis restricted to symmetric shapes have been performed for certain rare-earth and transition nuclei[10] and are themselves impressive in terms of effort and computer requirements, even with the relatively simple Skyrme III interaction employed. These calculations obviously can tell us nothing about the origin of asymmetric shapes and give limited insight into the structural origins of even axially symmetric shapes.

The present calculations are based on a more modest model, the self-consistent anisotropic oscillator (SCAO) model. The SCAO model gives substantially the same relative deformations as the HF method for light nuclei[11] and the relation between the predicted nuclear shape and which basis states are occupied is direct. The calculations are relatively easy to perform and require little computer time, since no iterative procedures are involved. This method is thus well adapted to mapping the trends in nuclear intrinsic shapes throughout the transition region to see if and where asymmetric shapes occur.

II. DESCRIPTION OF THE MODEL

The usual means of employing the anisotropic oscillator (AO) model is as a source of zero-order potential and basis states[5,6,7]. One diagonalizes a Hamiltonian that includes spin-orbit ($c\vec{\ell}\cdot\vec{s}$) and orbit-orbit ($D\ell^2$) corrections in addition to the three oscillator Hamiltonians corresponding to the coordinate directions. The deformed single particle states are then labeled by the total oscillator number N of a given shell, the orbital angular momentum ℓ, the spin (1/2), the total angular momentum j and its projection Ω on the body-fixed 3 axis. Instead

of true angular momenta, pseudo angular momenta ℓ_t, j_t and projection Ω_t are usually used, which are more easily constructed from pseudospace coordinates measured in units of the length parameters, e.g.

$$\xi^2 = \frac{m\omega_x}{\hbar^2} x^2 = x^2/b_x^2 .$$

The eigenvectors of the deformed Hamiltonian are linear combinations of these $|N\ell\frac{1}{2}j\Omega\rangle$ states, involving sums over j and, for axially asymmetric states, Ω.

Instead of following this approach, we evaluate the expectation value of the Hamiltonian between products of AO basis states (n_{xi}, n_{yi}, n_{zi}) such that $N = n_{xi}+n_{yi}+n_{zi}$. Since pure (asymptotic) asymmetric states are used, the nonaxial deformation will be larger than if the total Hamiltonian (which contains spin-orbit terms tending to favor a more spherical shape) were diagonalized. The nonaxial deformation should thus be as large as could reasonably be expected, and the overall deformation will be determined by which basis states (n_{xi}, n_{yi}, n_{zi}) are occupied. The requirement that an isopotential surface be an isodensity surface leads to the familiar result[12] that

$$\omega_x\Sigma_x = \omega_y\Sigma_y = \omega_z\Sigma_z = \omega_o\Sigma_A \qquad (3)$$

$$\text{so} \quad \langle H\rangle = \hbar\omega_x\Sigma_x + \hbar\omega_y\Sigma_y + \hbar\omega_z\Sigma_z = 3\hbar\omega_o\Sigma_A$$

$$\text{where} \quad \omega_x\omega_y\omega_z = \omega_o^3$$

$$\Sigma_x\Sigma_y\Sigma_z = \Sigma_A^3 \qquad (4)$$

and $\Sigma_x = \Sigma_{i=0}^{N_{max}} (n_{xi} + 1/2)$, with similar sums relating n_{yi} to Σ_y and n_{zi} to Σ_z. These results may also be obtained by minimizing $\langle H\rangle$ with respect to ω_x, ω_y, or ω_z with $\omega_o\Sigma_A$ as a Lagrange multiplier. The remaining requirement is then that the sets of basis states or "orbits" (n_{xi}, n_{yi}, n_{zi}) included in the ground state many particle wave function should be filled in such order as to minimize Σ_A. The scheme is then completely self-consistent. The energy $\hbar\omega_o$ is found from the binding energies of Os and Pt nuclei and a fit to their charge radii. The mean square neutron and proton radii were taken to be the same, but the ω_o's were different for neutrons than protons. The portions of the $\vec{\ell}\cdot\vec{s}$ and ℓ^2 terms diagonal in the Hamiltonian constitute corrections to the binding energy insufficient to change the level ordering with the parameters used here, which were $\hbar\omega_{on} = 7.50$ MeV, $\hbar\omega_{op} = 6.65$ MeV, $C = 0.2\ \hbar\omega_o$ and $D = 0.0045\hbar\omega_o$ (following the values recommended by Newton[13]).

If the total valence quanta are denoted by n_x, n_y, and n_z with $n_x+n_y+n_z = kN$, expansion of Σ_A^3 shows that minimizing H is equivalent to finding

$$\min\ [n_xn_yn_z - \tfrac{1}{2}(N_c+\tfrac{k}{2})\ (n_x^2+n_y^2+n_z^2)] \qquad (5)$$

Here N_c is the number of quanta in a particular rectangular coordinate direction summed over states in the core and k is the number of valence nucleons outside the closed core. The order of filling and emptying the N=4 and N=5 orbits according to this criterion is shown in Table I. Note that the symmetry axis shifts from the z to the y direction as the deformation goes from prolate to oblate. In practice the z axis is retained as the symmetry axis and the n_{zi} and n_{yi} values for the hole (unfilled) orbits are interchanged. The order of filling also requires $n_x \geq n_y$ (except where noted below), in order that the second order nonaxial moment Q_{22} be positive or zero.

Many of the structural features of the transition region are due to the fact that one has both N=4 and N=5 (h 11/2) partially filled proton subshells and N=5 and N=6 (i 13/2) partially filled neutron subshells. The present calculations use a particular set of orbits for the N=5 protons, permutations of (0,1,4). The orbits used for the N=6 neutrons are permutations of (0,2,4) and the (2,2,2) orbit. This choice gives the minimum values for the fourth order moments for ^{208}Pb; these moments cannot be made zero in the AO model. The second order moments of ^{208}Pb are all zero, however.

A portion of the calculations that is not completely self-consistent concerns the choice of the order in which the differing oscillator shells are emptied; because the expectation value of the spin-orbit term is taken for good AO states, rather than diagonalizing the entire Hamiltonian, the relative positions of the N=4 and N=5 proton and N=5 and N=6 neutron subshells are not fixed by the model. The choice of which subshell the next "orbital" is taken from is made to agree with the Nilsson orbitals[5]. The order of emptying the subshells is indicated in Table I. The order of emptying orbits within a given oscillator shell is self-consistent and follows the minimization procedure described above.

In the pure SCAO model, the region of oblate nuclei would extend through almost half the major oscillator shell being filled (N=4, protons; N=5, neutrons, see Table I) which is obviously contrary to experiment. In order to have the prolate-oblate transition occur in approximately the correct region, we minimize within each subshell such that for the prolate cases considered here, the protons and N=6 neutrons have $n_x \leq n_y$ and the N=5 neutrons $n_x \geq n_y$. The oblate cases have $n_x \geq n_y$ for both protons and neutrons, with all subshells similarly aligned.

This adjustment to the model produces the same variational energies as with the orbits not interchanged; the contributions

TABLE I. Order of neutron and proton orbit filling or emptying major shells. Note that rearrangement is required in the optimal configuration changes at the eleventh position (denoted by *). The number of protons or neutrons present at which a given orbit is filled is given for the cases studied.

(n_{xi},n_{yi},n_{zi})	(n_x,n_y,n_z)	$n_xn_yn_z$	$n_x^2+n_y^2+n_z^2$	Z
	N = 4 PROTONS			
(004)	(004)	0	16	
(103)	(107)	0	50	
(013)	(1,1,10)	10	102	
(202)	(3,1,12)	36	154	
(112)	(4,2,14)	112	216	
(022)	(4,4,16)	256	288	
(301)	(7,4,17)	476	354	
(211)	(9,5,18)	810	430	
(400)	(13,5,18)	1170	518	
(310)	(16,6,18)	1728	616	68
(121)	(17,8,19)	2584	714	70
(220)	(19,10,19)	3610	822	72
(031)	(19,13,20)	4940	930	76
(130)	(20,16,20)	6400	1056	80
(040)	(20,20,20)	8000	1200	82
	N = 5 PROTONS			
(104)	(104)	0	17	
(014)	(118)	8	66	
(401)	(519)	45	107	
(410)	(929)	162	166	66
(041)	(9,6,10)	540	217	74
(140)	(10,10,10)	1000	300	78
	N = 5 NEUTRONS			
(005)	(005)	0	25	
(104)	(109)	0	82	
(014)	(1,1,13)	13	171	

	(n_{xi},n_{yi},n_{zi})	(n_x,n_y,n_z)	$n_xn_yn_z$	$n_x^2+n_y^2+n_z^2$	N
		N = 5 NEUTRONS			
	(203)	(3,1,16)	48	266	
	(113)	(4,2,19)	152	381	
	(023)	(4,4,22)	352	516	
	(302)	(7,4,24)	672	631	
	(212)	(9,5,26)	1170	782	
	(122)	(10,7,28)	1960	933	
	(032)	(10,10,30)	3000	1100	
*	(401)	(14,10,31)	4340	1257	
*	(311)	(21,6,28)	3528	1261	
	(410)	(25,7,28)	4900	1458	
	(122)	(26,9,30)	7020	1657	104
	(221)	(28,11,31)	9548	1866	106
	(320)	(31,13,31)	12493	2091	108
	(032)	(31,16,33)	16368	2306	116
	(131)	(32,19,34)	20672	2541	118
	(230)	(34,22,34)	25432	2796	120
	(041)	(34,26,35)	30940	3059	122
	(140)	(35,30,35)	36750	3350	124
	(050)	(35,35,35)	42875	3675	126
		N = 6 NEUTRONS			
	(204)	(204)	0	20	
	(024)	(228)	32	72	
	(402)	(6,2,10)	120	140	
	(222)	(8,4,12)	384	224	
	(042)	(8,8,14)	896	324	110
	(420)	(12,10,14)	1680	440	112
	(240)	(14,14,14)	2744	588	114

to the energy from the neutron and proton shape terms are the same, and the spin-orbit contribution is symmetric with respect to the interchange of x and y. In nature, the interaction between neutrons and protons would cause their densities to be more similar in shape than allowed by our model, which only correlates the two types of nucleons through the choice of a common reference frame. This applies to both oblate and prolate densities, since the two types of nucleons fill different single-particle states. The orientation adjustment for the prolate case corrects the overall particle density for neglect of the rounding effects produced by the n-p correlations and the pairing correlations between like nucleons. Filling the oscillator configuration pairwise (except for the unpaired proton in Ir and Au) also accounts for some of the pairing tendency.

III. RESULTS OF THE CALCULATION

As measures of deformation we take the second and fourth order mass multipole moments of the nuclei:

$$Q_{20} = \langle z^2 - x^2/2 - y^2/2 \rangle$$

$$Q_{22} = (3/2)^{1/2} \langle x^2 - y^2 \rangle \qquad (6)$$

$$Q_{40} = \langle z^4 + \tfrac{3}{8}(x^4 + y^4) - 3(x^2z^2 + y^2z^2) + \tfrac{3}{4}x^2y^2 \rangle$$

$$Q_{42} = (5/8)^{1/2} \langle y^4 - x^4 + 6z^2(x^2 - y^2) \rangle$$

$$Q_{44} = (35/32)^{1/2} \langle x^4 + y^4 - 6x^2y^2 \rangle$$

where the pointed brackets indicate expectation values taken with respect to the ground state. The values of the second order moments (in fm^2) and the fourth order moments (in fm^4) are given in Table II for the following nuclei studied: $^{178-188}W$, $^{182-194}Os$, $^{187-195}Ir$, $^{186-198}Pt$, $^{191-199}Au$, and $^{194-206}Hg$.

It is customary to analyze experimental reaction information in terms of a nuclear radius proportional to V_2+V_4 of (1) and (2). This may be a sharp cutoff radius for a constant-density volume distribution or just an isodensity contour. To first order, one has the coefficients of Y_{LO} or $Y_{LM} + Y_{L,-M}$ (excluding k_2) are

$$\frac{(2L+1)^{1/2}\,(4\pi)^{1/2}\,Q_{LM}}{3A\langle r^2\rangle_{mean}^{L/2}} \qquad (7)$$

from evaluating Q_{LM} for a sharp cutoff density distribution. Approximations in both the structure model and experimental analysis render fruitless the attempt to provide a connection between these two descriptions of deformation beyond first order. The prescription (7) gives reasonable estimates of

$$\gamma = \tan^{-1}[(2)^{1/2}Q_{22}/Q_{20}]$$

$$\beta_2 = (2.64222Q_{20})/(A\langle r^2\rangle_M \cos\gamma) \qquad (8)$$

$$\beta_4 = (3.54491Q_{40})/(A\langle r^2\rangle_M^2)$$

These quantities are also given in Table II. The values of γ range from 0 to $\pi/6$; β_2 is positive for predominantly prolate nuclei, and negative for predominantly oblate nuclei.

Since the neutron and proton moments differ more widely in this model than is expected to be the case in nature, we recommend that the overall moments multiplied by Z/A be used to represent the charge moments of these nuclei. This is one of the reasons for not listing the neutron and proton moments separately.

Referring to Table II, it can be seen that the predicted axial deformations (β_2 and β_4) are in reasonably good accord with both experiment[15] and other predictions[4,8]. W, Os, and Ir nuclei display a prolate-oblate transition between N=112 and N=114 and all Pt, Au, and Hg nuclei are predicted to be oblate ($\beta_2<0$). The trend of decreasing $|\beta_2|$ with increasing neutron number is also reproduced. All nuclei studied (except ^{186}Pt) have rather large negative β_4 deformations. We have also established that in our model the transition to positive hexadecapole moments occurs near ^{168}Er. Differences between predicted magnitudes of β_2 and β_4 and measured deformations are probably due as much to the approximation made in extracting these quantities from the mass moments (eq. (7)) as to deficiencies in our model.

A comparison of the model $|\beta_2|$ values with experiment is shown in FIG. 1. The experimental values are from the compilation of Grodzins and Stelson[15]. The trends and even the magnitudes of $|\beta_2|$ are reasonably well reproduced. The systematic tendency of the model results to be slightly too small for the prolate case and somewhat too large for the oblate case probably stems from the fact that the orientation adjustment used in the model partially compensates for the neglect of short range correlation effects in the prolate case and not in the oblate case.

Examination of the asymmetry angle γ of Table II reveals that the largest asymmetries occur mainly for N=110, 112 on the prolate side of the transition and for N=116, 118 on the oblate side. It is noteworthy that the oblate nuclei just after transition (^{188}W, ^{190}Os, ^{191}Ir, $^{188,190,192}Pt$) have small predicted asymmetries γ. With the exception of the N=114 isotones, the Os and Ir isotopes are all predicted to have relatively large asymmetries. Contributions to asymmetric shapes from the fourth-order moments Q_{42} and Q_{44} are quite large; with very few exceptions, at least one of these moments is predicted to be large for all nuclei studied. Such large L=4 asymmetries can be expected to have non-negligible effects on both the energy spectra and the transition rates for nuclei in this mass region.

IV. DISCUSSION

The model used here was chosen such as to allow for possible triaxial distortion, a reasonable fit to the prolate-oblate transition, and some measure of self-consistency. On the positive side, its main parameters used here were found by straightforward procedures in common use[5,13], and yield moments comparable to the best available Hartree-Fock calculations[10].

Such a simple model as ours must incorporate approximations that would be considered excessive in more refined models. In order of roughly decreasing importance, these are: (a) the treatment of neutrons and protons separately,

TABLE II. Quadrupole and hexadecapole axial and nonaxial moments for the transition nuclei. The sharp cut-off distortions β_2 and β_4 are first-order approximations (see text). The asymmetry parameter γ is given to the same order.

Nucleus	Q_{20}^{2}(fm)	Q_{22}^{2}(fm)	Q_{40}^{4}(fm)	Q_{42}^{4}(fm)	Q_{44}^{4}(fm)	β_2	γ	$\beta_4(10^{-2})$
$_{74}W_{104}$	589.3	20.3	-2700.6	-1375.4	2485.9	0.263	2.8°	-4.868
$_{74}W_{106}$	565.6	19.0	-3391.7	-1258.1	1418.2	0.250	2.7°	-6.044
$_{74}W_{108}$	506.5	9.7	-3248.0	789.6	134.89	0.221	1.5°	-5.727
$_{74}W_{110}$	503.8	114.3	-4197.3	3042.9	1936.1	0.228	17.8°	-7.261
$_{74}W_{112}$	435.9	65.8	-3828.2	2833.6	-204.7	0.190	12.0°	-6.545
$_{74}W_{114}$	-656.1	0.0	-4344.6	0.0	-13044.8	-0.276	0	-7.334
$_{76}Os_{106}$	555.7	68.9	-4099.1	2354.5	1154.6	0.247	10.0°	-7.250
$_{76}Os_{108}$	496.6	97.62	-3955.4	1886.0	-128.8	0.223	15.5°	-6.923
$_{76}Os_{110}$	426.0	153.7	-4531.8	3942.1	-459.5	0.202	27.0°	-7.651
$_{76}Os_{112}$	426.0	153.8	-4535.6	3930.0	-468.3	0.202	27.0°	-7.699
$_{76}Os_{114}$	-632.7	64.8	-2482.0	2056.8	-4121.4	-0.266	8.2°	-4.150
$_{76}Os_{116}$	-590.5	121.3	-3393.6	3407.3	-3811.3	-0.253	16.2°	-5.617
$_{76}Os_{118}$	-547.9	121.0	-4276.9	3458.2	-4149.4	-0.234	17.3°	-7.008
$_{77}Ir_{110}$	431.1	109.6	-4192.7	3417.8	-382.0	0.194	19.8°	-7.139
$_{77}Ir_{112}$	431.1	109.7	-4196.5	3405.7	-390.8	0.193	19.8°	-7.184
$_{77}Ir_{114}$	-590.9	48.0	-2728.5	1527.6	-4188.9	-0.246	6.6°	-4.538
$_{77}Ir_{116}$	-548.7	104.6	-3640.1	2878.1	-3878.8	-0.233	15.1°	-5.994
$_{77}Ir_{118}$	-506.1	104.3	-4523.4	2929.0	-4216.9	-0.214	16.2°	-7.374
$_{78}Pt_{108}$	-674.7	148.1	-271.8	1465.5	-6193.4	-0.301	17.2°	0.467
$_{78}Pt_{110}$	-674.6	31.7	-572.2	945.7	-4953.6	-0.285	3.8°	-0.968
$_{78}Pt_{112}$	-612.0	25.8	-1794.7	824.8	-4571.2	-0.255	3.4°	-3.003
$_{78}Pt_{114}$	-548.7	31.7	-2871.1	945.7	-4247.0	-0.227	4.7°	-4.748
$_{78}Pt_{116}$	-506.5	88.2	-3782.7	2296.3	-3936.9	-0.213	13.8°	-6.194
$_{78}Pt_{118}$	-463.9	87.9	-4666.1	2347.2	-4275.0	-0.194	15.0°	-7.565
$_{78}Pt_{120}$	-421.0	31.7	-5473.4	945.7	-4012.7	-0.169	6.1°	-8.784
$_{79}Au_{112}$	-581.7	41.8	-1986.2	1281.8	-4609.4	-0.242	5.8°	-3.309
$_{79}Au_{114}$	-518.4	15.7	-3062.6	488.6	-4285.1	-0.213	2.5°	-5.043
$_{79}Au_{116}$	-476.2	72.3	-3974.2	1839.2	-3975.0	-0.198	12.1°	-6.479
$_{79}Au_{118}$	-433.6	71.9	-4857.6	1890.1	-4313.1	-0.179	13.2°	-7.840
$_{79}Au_{120}$	-390.7	15.7	-5664.9	488.6	-4050.8	-0.156	3.3°	-9.052
$_{80}Hg_{114}$	-487.9	0.0	-3212.2	0.0	-4316.8	-0.199	0	-5.264
$_{80}Hg_{116}$	-445.7	56.6	-4123.8	1350.5	-4006.7	-0.183	10.2°	-6.692
$_{80}Hg_{118}$	-403.1	56.2	-5007.1	1401.4	-4344.8	-0.164	11.1°	-8.045

Table II. (continued)

Nucleus	Q_{20}^{2}(fm)	Q_{22}^{2}(fm)	Q_{40}^{4}(fm)	Q_{42}^{4}(fm)	Q_{44}^{4}(fm)	β_2	γ	$\beta_4(10^{-2})$
$_{80}Hg_{120}$	-360.2	0.0	-5814.4	0.0	-4082.5	-0.143	0	-9.248
$_{80}Hg_{122}$	-284.8	27.7	-5960.1	1116.8	-3961.6	-0.113	7.8°	-9.389
$_{80}Hg_{124}$	-208.7	0.0	-5949.1	0.0	-3854.8	-0.081	0	-9.278
$_{80}Hg_{126}$	-98.8	0.0	-4373.3	0.0	-3708.4	-0.038	0	-6.748
$_{82}Pb_{126}$	0.0	0.0	-3173.4	0.0	-3792.9	0.0	0	-4.851

(b) the use of pure AO single particle states, (c) prolate shapes are stabilized by choosing Q_{22} to differ in sign for neutrons and protons respectively, (d) the choice of the N=5 proton and N=6 subshells was made so as to make the second order moments of ^{208}Pb to be zero, and the fourth order moments as small as possible (subject to criteria (b) and (d), this choice is unique), (e) the order of emptying subshells (but not levels) conforms to the Nilsson model.

As is customary, we argue that effects on the moments due to neglecting the neutron-proton interaction should be small since we are filling different oscillator shells in each case. We also think that such effects (a) will be accounted for in part by choices (c), (d), and (e).

The reason for not diagonalizing the Hamiltonian (mixing the basis states (b)) is that this would prevent us from using

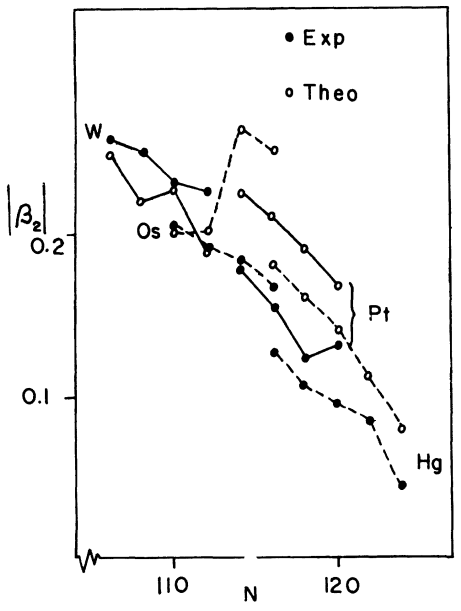

FIG. 1. Absolute values of β_2 as a function of neutron number N. Theoretical values (open circles) from the SCAO model are compared with experimental values (solid circles) from the compilation of Stelson and Grodzins[15]. The lines are drawn merely to guide the eye.

the self-consistency requirement to determine the shapes. The neglect of the effect of short-range correlations introduces an error whose size is subject to dispute. This type of correlation is usually put in via the use of an explicit pairing Hamiltonian to mock up the effect of the short range part of the nuclear interaction. It has been argued[16] that the true short range correlation should have little effect on the equilibrium shape determination, whereas use of the pairing force definitely tends to produce shapes that favor prolate distortions and smaller nonaxial moments[4]. It has also been shown that reasonable values of moments of inertia for rare-earth nuclei may be obtained without the use of the pairing correction term[17]. It seems that short range correlations are also included in the field-producing terms, so that explicit use of the pairing force or use of Hartree-Fock-Bogoliubov (HFB) in place of Hartree-Fock (HF) methods includes some of the short range effects twice. We think our calculations give a practical lower limit on the effects of short-range correlations. A practical upper limit is probably given by explicit use of the pairing force[7]. It seems to us that overall agreement of a model including the effects of fourth order deformations with experimental transition rates and spectra throughout the entire region would be necessary to determine the optimum mixture.

The effects of the choice of subshell orbits to minimize fourth order moments in Pb are compensated to a certain extent by requirement (c) that the prolate-oblate transition indeed take place in the transition nuclei. As mentioned earlier, an unknown amount of pairing effect is also absorbed in this fashion. As far as the shapes are concerned, assumptions (a), (c) and (d) tend to produce effects that cancel each other. Assumption (e) is inherently reasonable and produces results in agreement with other calculations[6].

The stability of these shapes is essentially given by the difference in energy between two configurations that differ only in which orbits are filled. This ranges from 20 to 200 MeV, depending on N and Z. Orbits equivalent up to interchange of n_x and n_y are of course degenerate. Within the model, then, the shapes are stable. However, for small γ (say,

less than 10°) the shapes can be considered essentially axially symmetric, since only small perturbations would be necessary to produce symmetry. For small γ, there is negligible difference between the asymmetric rotor spectra and an axially symmetric model employing γ-vibrations[6].

The agreement between our results for γ and its extraction from spectral information is sometimes good, sometimes bad, depending on the nucleus. For example, we obtain around 27° for the value of γ for ^{186}Os, whereas the value from spectral information is about 16°. In view of the fact that fourth order deformations are ignored in finding γ from experimental spectra it seems to us that the question of how asymmetric the transition nuclei are is still open.

In summary, we find a structural basis exists for possible asymmetric shapes in the transition region, particularly for the Os nuclei, for ^{189,193,195}Ir, for ^{194,196}Pt, and for ^{195,197}Au. These nuclei have sizeable fourth-order moments that should not be neglected in extracting the shape parameters from experimental information. For most of the transition nuclei, the asymmetries found by our model are small enough that dynamical models other than the triaxial rotor[18,6,19] would provide equally adequate spectra and transition rates. Thus, the degree to which the triaxial rotor model provides a uniquely good description of the transition nuclei has yet to be determined by spectral calculations including fourth order deformations.

ACKNOWLEDGEMENTS

This work was completed while the author was on sabbatical leave at the University of Georgia. He thanks John Henkel and George Strobel for hospitality, and F. Todd Baker for computer time and instruction on the experimental results on nuclear shapes in the transition region.

[1] J. Meyer ter Vehn, F. S. Stephens, and R. M. Diamond, Phys. Rev. Lett. 32, 1383 (1974); J. Meyer ter Vehn, Nucl. Phys. A249, 111 (1975); ibid, A249, 149 (1975); Phys. Lett. 55B, 273 (1975); E. F. Zganjar, J. L. Wood, R. W. Fink, L. L. Riedinger, C. R. Bingham, B. D. Kem, J. L. Weil, J. H. Hamilton, A. V. Ramayya, E. H. Spejewski, M. L. Mlekodaj, H. K. Carter, and W. D. Schmidt-Ott, Phys. Lett. 58B, 159 (1975).

[2] H. Toki and A. Faessler, Nucl. Phys. A253, 231 (1975); A. Faessler and H. Toki, Phys. Lett. 98B, 211 (1975).

[3] F. Todd Baker and D. Goss, Phys. Rev. Lett. 36, 852 (1976).

[4] K. Kumar and M. Baranger, Nucl. Phys. A122, 241 (1968); ibid, A122, 273 (1968); ibid, A92, 608 (1967).

[5] B. R. Mottleson and S. G. Nilsson, K. Danske Vidensk. Selsk. mat.-fys. Skr. 1, No. 8 (1959).

[6] K. T. Hecht and G. R. Satchler, Nucl. Phys. 32, 286 (1962).

[7] I. Ragnarsson, A. Sobiczewski, R. K. Sheline, S. E. Larsson, and B. Nerlo-Pomorska, Nucl. Phys. A233, 329 (1974).

[8] U. Götz, H. C. Pauli, K. Alder, and K. Junker, Nucl. Phys. A192, 1 (1972).

[9] A. S. Davydov and G. F. Filippov, Nucl. Phys. 8, 237 (1958).

[10] H. Flocard, P. Quentin, and D. Vautherin, Phys. Lett. 46B, 304 (1973); M. Cailliau, J. Letessier, H. Flocard, and P. Quentin, A. K. Kerman, and D. Vautherin, Nucl. Phys. A203, 433 (1973).

[11] D. Goss, Phys. Rev. C 2, 1168 (1970).

[12] B. R. Mottelson, in Lectures at the Ecole d'Ete'de Physique Theórique, Les Houches (Paris, 1958).

[13] T. D. Newton, Can. J. Phys. 38, 700 (1960).

[14] F. T. Baker, T. H. Kruse, W. Hartwig, I. Y. Lee, and J. X. Saladin, Nucl. Phys. A258, 43 (1976).

[15] C. E. Bemis, Jr., P. H. Stelson, F. K. McGowan, W. T. Milner, J. L. C. Ford, Jr., R. L. Robinson, and W. Tuttle, Phys. Rev. C 8, 1934 (1973); I. Y. Lee, J. X. Saladin, C. Baktash, J. E. Holden, and J. O'Brien, Phys. Rev. Lett. 33, 383 (1974); W. Bruckner, D. Husar, D. Pelte, K. Traxel, M. Samuel, and V. Smilansky, Nucl. Phys. A231, 159 (1974); ref. (14); P. H. Stelson and L. Grodzins, Nucl. Data 1, 21 (1965).

[16] M. A. Preston, Physics of the Nucleus (Addison-Wesley, 1962) 272.

[17] S. K. M. Wong, M. I. Tienhaara, and L. E. H. Trainor, Phys. Rev. Lett. 21, 1819 (1968).

[18] T. Tamura and T. Udagawa, Nucl. Phys. 16, 460 (1960).

[19] M. Baranger and K. Kumar, Phys. Lett. 17, 1146 (1966).